*Submitted to* ***Earth Surface Processes and Landforms***

August 16, 2001

# LONG RUN-OUT MASS MOVEMENTS IN GLACIALLY CONDITIONED LANDSCAPES

Kyle K. Nichols
802 656 3398 (voice)
802 656 0045 (fax)
kknichol@zoo.uvm.edu

Paul R. Bierman

School of Natural Resources and Department of Geology, University of Vermont, Perkins Hall, Burlington, VT 05404 USA

Keith Klepeis
Stephen F. Wright
Milo Peavey
Megan McGee

Department of Geology, Perkins Hall, University of Vermont, Burlington, VT 05405 USA

**ABSTRACT**

Landslides are common in glacially conditioned landscapes characterized by fine-grained glacial sediment. Normally, these landslides are initiated by heavy rainfall, rapid snowpack melting, or bank undercutting, and have hazard zones that are limited in extent. In April 1999, three landslides (4,300 $m^3$ to 23,000 $m^3$) in glaciolacustrine sediments at Jeffersonville, Vermont, fell ~ 46 m, mobilized, and ran out 290 m. The long runout was enabled by the rapidly deforming basal 20 cm of slide debris, a liquefied shear zone. Mud volcanoes on the debris surface suggested that the landslide debris was saturated during and after deposition.

The Jeffersonville landslide is unusual because it occurred during a spring with normal to below normal precipitation. Neither heavy rainfall nor bank undercutting was the immediate cause of landsliding. Heavy rainfall in the summer of 1998 (175% of normal) appears to have had a delayed effect on the deep bedrock groundwater system feeding the slide. There was a six to eight month lag in pore pressure response from the upland recharge zone to the valley where the landslides occurred.

Analysis of the Jeffersonville landslide has important implications for hazard prediction where silt and clay are common. Runout zone prediction should consider possible landslide mobilization and resultant runout lengths up to an order of magnitude longer than the drop. Potentially unstable slopes, adjacent to high topography, may be hazardous for months after prolonged heavy rainfall due to a lag in pore pressure response.

**INTRODUCTION**

Glacially conditioned landscapes dominate the high latitudes. In these areas, landslides commonly occur in glacially deposited materials including fine-grain glacial lake and glacial marine sediment (Mollard, 1977; Niini and Slunga, 1989; Viberg, 1989). Slope instability is often triggered by increasing pore pressure, or by oversteepening caused by Holocene processes, such as riverbank incision or human excavation, which modify glacial landscapes (Braun *et al*., 1989). Many regions once occupied by glaciers, such as the northeastern United States and much of Europe, are heavily populated and thus landslides in glacial sediments pose a significant geologic hazard (Brabb, 1989).

Landslides in glaciated terrains come in all sizes from rare but massive failures that displace millions of cubic meters of sediment (e.g., the Nicolet, Quebec, and the South Nation River, Ontario earthflows; Mollard, 1977) to inconsequential slips that move a few cubic meters of material down streambanks. The large mass movements are typically rigid, slowly and sequentially mobilizing masses of debris that may flow long distances from the source (Mollard, 1977). In contrast, the most common landslides in glaciated terrains, those along river and stream banks, typically move only short distances from their source allowing easy and rapid delineation of hazard zones (Braun *et al.*, 1989; Viberg, 1989).

In this paper, we report data indicating that long runout landslides in glacial sediment may be a significant geologic hazard. We document a landslide complex along the Brewster River in Jeffersonville, Vermont (Figure 1), where more than 27,000 $m^3$ of material moved down slope, crossed a river at the toe of the slide, partially liquefied, and thus, being highly mobile, spread out over the distal floodplain much farther than previous hazard predictions would have suggested. The slide is particularly interesting because it occurred during a season when precipitation was average to below average. The Jeffersonville landslide complex has implications for other glacially conditioned landscapes because is suggests that hillslopes may fail months after heavy rainfall, partially liquefy, and runout long distances thus making it difficult to predict the extent, timing, and location of such failures.

## GEOLOGIC SETTING

More than 14,000 years after continental ice sheets ablated, the effects of glaciation and glacial sediment still shape landscapes and influence surface processes in mid- and high-latitudes. Thirteen to fourteen thousand years ago, the site of the Jeffersonville landslides was 50 to 150 m below several ice-dammed lakes. These lakes and many others along the retreating Laurentide margin were sinks for fine-grain material washing off of hillslopes and out of the ablating ice (Chapman, 1937). A coarsening upward sequence of sand over silt, such as observed at Jeffersonville, is common throughout glaciated regions as glacial lake levels lowered and deltas prograded (Koteff and Pessell, 1981). These stratigraphic sequences are commonly associated with slope instability (Dunne and Leopold, 1978).

The stratigraphy of the failed bank, at Jeffersonville, is dominated by alternating silt and clay or sand and clay couplets. In total, there are more than 143 exposed couplets. The couplets coarsen and thicken upward; fine and medium sand replace the silt. These glaciolacustrine sediments are capped by up to 5 m of fluvial sand and gravel. The thickness of the clay layers ranges from 0.4 cm to 2.9 cm and the thickness of the silt layers ranges from 6.7 cm to 52 cm. There are two sections where silt/clay couplets are convoluted, faulted, and abnormally thick suggesting soft-sediment deformation by sub-aqueous slumping just after deposition. The lower section of convoluted beds, 5 m above the river, forms a prominent bench in the slide scar and can be traced morphologically into the adjacent hillslope. Joints, many of which exhibit iron oxide staining, cut the more

clay-rich layers, suggesting that groundwater flow in the fine-grain material is controlled at least in part by secondary porosity.

## METHODS

We used a Trimble 4400 differential Global Positioning System (accurate to a few centimeters) to survey the landslide debris in detail. We surveyed >3,000 points to delineate the debris topography, tree orientation, slide margin, and floodplain topography. Because of the unstable slope, we collected only enough points to delineate gross topography of the landslide scarp. Topographic maps and volume calculations were made with Surfer® software.

We adapt the $R_f/\phi$ technique of fabric analysis (Lisle, 1985), originally developed by structural geologists to quantify tectonic strain in ductilely deformed rocks, to measure the preferred orientation and three-dimensional shape of deformed and rotated clay clasts in the basal layer of the debris. We use these data to illustrate the close relationship between transport and emplacement of the landslide debris and the development of an anisotropic grain shape fabric during fluidized shear at the base of this debris.

We used two methods to determine shear strength of material cropping out in the scarp. We used direct shear tests to measure soil cohesions and internal friction angles of vertically collected sediment samples from three sites: below the prominent bench, on the bench, and above the bench. We used these parameters in the Bishop method of slices (Bishop, 1955), to estimate the hillslope saturation at failure. We also conducted vertical and horizontal shear vane tests *in situ* to measure soil cohesions of the lower 15-m of the

glacial clay and slit. We assumed soil cohesion of the overlying sand and gravel was approximately zero.

## SLIDE HISTORY

During the spring and summer of 1999, a 46-m high bank of the Brewster River failed and produced three large and exceptionally mobile landslides (Figure 2). All three landslides moved down the steep slope, across the Brewster River, and onto the flood plain beyond. The first landslide occurred on April 11, 1999; the second and largest landslide occurred on April 18, 1999, and the third landslide occurred on July 4, 1999. The combined volume of the first and second slides, based on high resolution (<5 centimeter precision) Global Positioning System (GPS) mapping after the second slide, was ~23,000 $m^3$; we estimate an additional 3,000 $m^3$ was excavated by the Brewster River immediately after the slide. The third slide contributed another 4,300 $m^3$ of debris. The largest slide traveled ~290 m across the channel and adjacent floodplain of the Brewster River (Figure 3). Slide debris covered 31,400 $m^2$ of Brewster River floodplain and terraces to an average thickness of 0.7 m; the thickest deposits exceeded 4 m (Figure 3).

Landslides are common and frequent along the reach of the Brewster River where the 1999 landslides occurred. Historic photographs from the early 20$^{th}$ century document that sliding and slumping were common almost a century ago (Figure 2A). Aerial photographs taken in 1962 show that a landslide crossed the river and deposited abundant fine-grained material ~100 m north of the 1999 landslide sequence (Figure 1). Aerial photographs taken in 1974, 1979, 1988, and 1995 show various regions of the riverbank

devoid of trees, consistent with on-going, small-scale slope instability, but no exceptionally large landslides. Numerous revegetated landslide scars are visible both upstream and downstream of the 1999 slide location (Figure 1).

**RUNOUT ZONE**

The runout zone was a jumble of trees, blocks of intact silt and clay couplets (up to 10 $m^3$), gray mud, and numerous mud volcanoes (Figure 4). After the second slide, the runout zone had many characteristics of debris flows, including superimposed debris flow snouts (<1 m high) at the slide apron margin (Figure 3). The orientation of felled trees transported on the debris was bimodal (Figure 5). Most trees within 20 m of the slide margin were oriented parallel to local margin orientations, pushed along by the moving debris; most trees more than 20 m from the slide margin were aligned parallel to radial flow paths (Figure 5).

The original stratigraphy of the pre-slide material was generally preserved in the runout zone; the farthest traveled material was silt and clay from the bottom of the failed section whereas sand and gravel from the top of the section did not travel much beyond the base of the slide scar. Field observations, after the second and largest landslide, indicate that the Brewster River was blocked. However, the high-water marks indicate that backwater flooding never exceeded bankfull level. Because sand (not silt and clay) filled the channel, the river recut a channel before flooding occurred upstream.

*Evidence for debris flow-like behavior*

The second Jeffersonville landslide exhibited several features suggesting that it behaved like a debris flow in the runout zone. The long runout length, the mud volcanoes,

and the superimposed lobes of fine-grained material with steep noses at the slide margin (Figure 3), all suggest that the slide debris flowed across a nearly horizontal terrace. As the debris moved across the terrace, the basal layer of the debris liquefied from high pore pressures and allowed for the long runout. As the slide margins were unable to spread out farther, the more liquefied center continued to move and formed superimposed lobes (Figure 3). After the debris came to rest, the high pore pressures forced the water to the surface creating the mud volcanoes. The Jeffersonville slide is not unique. Many saturated or partially saturated landslides that move down steep (>3°) hillslope channels transform into debris flows (Bathurst *et al.*, 1997; Flemming *et al.*, 1989; Iverson *et al.*, 1997; Johnson, 1984).

*Debris runout length*

A striking feature of the Jeffersonville slide is the runout length in comparison to the height. *Runout length* can be defined as either the maximum travel length of debris or the center-of-mass travel length (Campbell *et al.*, 1995; Figure 6). Similarly, *height* can be defined as the maximum vertical elevation drop or the center-of-mass elevation drop. Since it is difficult to establish the center of mass in most large landslides, the maximum elevation drop and maximum travel lengths are commonly considered (Bathurst *et al.*, 1997; Campbell, 1989; Kilburn and Sørensen, 1998; Nayashi and Self, 1992). The Jeffersonville landslide had a maximum travel length of 290 m and a maximum head drop of 46 m.

One can use two different sets of empirical equations to estimate runout length. Because the Jeffersonville landslide complex has blocky debris and unconfined runout,

similar to landslides, landslide-based empirical equations seem reasonable to predict runout. Alternatively, the superimposed snouts at the slide margin and the liquefied debris are representative of debris flow runout; thus, debris-flow-based empirical equations might be useful to predict runout length.

Although it is difficult to predict the runout potential of landslides, landslide volume and runout distances are generally well-correlated (Kilburn and Sørensen, 1998). As slide volume increases for non-saturated, granular landslides, height/runout length (H/L) decreases; runout length increases faster than fall height (Campbell, 1989; Campbell *et al.*, 1995; Dade and Huppert, 1998; Kilburn and Sørensen, 1998; Nayashi and Self, 1992). This non-linear relationship of increasing runout length with increasing volume is observed for landslides on the Moon, Mars, and Earth (Campbell *et al.,* 1995; Kilburn and Sørensen 1998; Figure 7).

The second and largest Jeffersonville slide had a volume of $>10^4$ $m^3$ and an H/L ratio of 0.16 (center of mass H/L of 0.14) (Figure 7). Granular landslides of similar size ($\leq 10^5$ $m^3$) have H/L ratios that range from 0.35 to 0.65 (Campbell *et al.*, 1995; Dade and Huppert, 1998; Kilburn and Sørensen, 1998). Using an H/L ratio of 0.35 to predict the farthest runout still underestimates the actual runout length by more than 50% (130 m compared to 290 m; Table I).

Alternatively, empirical equations that predict debris flow runout lengths mostly overestimate the runout length of the second Jeffersonville slide (Table I). The predicted runout and the measured runout at Jeffersonville differ because the debris flow empirical data are based on individual debris flows moving down gullies or down experimental

flumes (Bathurst *et al.*, 1997; Iverson *et al.*, 1997). Such confined debris flows do not represent the unconfined Jeffersonville debris that spread across the low gradient floodplain of the Brewster River.

Neither, the landslide nor the debris flow runout equations predict well the Jeffersonville landslide runout. Some granular landslides (e.g. Blackhawk landslide in California) have long runout distances due to large volumes and vibrational energy creating a low frictional shear zone at the base of the slide material (e.g. Hsü, 1975; Campbell, 1989; Campbell *et al.*, 1995). The Jeffersonville slide complex, however, has a relatively small volume and is not entirely granular; it is at least partially saturated silt and clay. Like large granular landslides, the Jeffersonville landslides might have had increased vibrational energy during landsliding, which could have increased pore pressures to create the liquefied basal shear zone we observed (Iverson *et al.*, 1997; Major and Iverson, 1999). Such a liquefied basal zone appears to promote runout length longer than expected for granular landslides, but shorter than for channelized debris flows.

*Analysis of grain anisotropy in the basal shear zone*

We examined grain shape anisotropy and clast deformation in part of the basal shear zone when the State of Vermont removed all 27,000 $m^3$ of slide debris. Soft-sediment folding and faulting provided evidence of deformation during debris transport and the occurrence of mud volcanoes provided evidence of fluidisation of sediment possibly from a liquefied basal shear zone. Excavation indicated that landslide debris was in sharp contact with the underlying grass, indicating that material moved across the ground surface non-erosively (Figure 8A). Coherent blocks of landslide debris, above the

lowermost 20 cm of the deposit, exhibited the stratigraphy of the original silt and clay layers, although some sections were folded and faulted. In the 20-cm-thick basal zone, individual, mechanically stronger blocks of clay, 1 to 3 cm long, apparently derived from the original glacial lake sediments, were surrounded by a fine-grained, homogeneous, gray silt matrix (Figure 8A). These clasts displayed rounded, rectangular, and elliptical shapes and variable degrees of preferred orientations. These features were restricted to the 20-cm thick basal layer.

The excellent exposure and abundance of clay clasts allowed us to evaluate grain shape anisotropy within the basal layer and compare the properties of this fabric with the transport properties of the landslide. We measured the axial orientations ($\phi$) and aspect ratios ($R_f$) of over 80 clay clasts on three vertically oriented planes perpendicular to the horizontal flow plane. The first plane (12 measurements) was oriented almost parallel to the westerly flow direction (striking 085°), the second plane (38 measurements) was oriented perpendicular to the flow direction (striking due north), and the third plane (31 measurements) was oriented oblique to the flow direction (striking 326°). A statistical analysis of the data allowed us to evaluate whether clast rotation, clast shape change, or both processes produced the grain shape fabric during transport of the landslide debris. Best-fit curves for the data on each face were determined using the statistical methods described by Lisle (1985) and De Paor (1988). The average best-fit three-dimensional shape and orientation of the clasts were determined by combining the harmonic mean of ellipses found for each of the three planes according to the least squares method described

by Owens (1984). The number of measurements we used exceeded the minimum number of data per face recommended by Lisle (1985).

The results show that the strongest degree of preferred orientation of clasts occurs in the plane oriented parallel to or nearly parallel to the flow direction (plane 1). This is indicated by the lower degree of dispersion of the data along the $\phi$-axis in plane 1 (Figure 8B) compared to the other two planes. Plane 3 showed ellipses with the longest average axis (Figure 8B). The shape of the best-fit three-dimensional ellipsoid for the three planes indicates that the average shape of the clasts ($R_f$) was slightly prolate with near equal b and c axes ($R_s$ = 1.62 and 1.78, respectively) and a longer a axis ($R_s$ = 2.02). The trend of the longest axis (a) of this ellipsoid forms an angle of 52° clockwise from the westerly transport direction in a horizontal plane (Figure 8C). The other two axes of the best-fit ellipsoid (b, c) define a plane oriented obliquely to the transport direction. In addition, the average orientation of the long axes of the clasts is inclined upstream by ~27° (Figure 8C, D).

The similar clast axial ratios and $R_s$ values we obtained suggest that clast reorientation within a fluidized matrix during transport likely produced the preferred grain alignment. The slightly prolate shape could have resulted from either an original shape fabric that reflects the pre-existing clay layers from which the clasts were derived, or a small amount of shape change by deformation during flow. Hence, we suggest that the final shapes of the clasts mostly reflect their origin from nearby horizontal clay layers.

Despite this likelihood, however, all of our analyses passed the $I_{sym}$ test (0.84 to 0.92), suggesting a homogeneous initial distribution of clasts.

Current-produced imbrication is one of the most common types of grain shape anisotropies although the exact configuration depends on the mode of sediment transport and deposition. In gentle, bedload transport where grains roll or slide, grains typically lie with their long axes (a) oriented normal to flow and with the b-c planes inclined upstream (Leeder, 1982). However, during stronger flows, the long axis tends to parallel the flow direction. This latter configuration best conforms to our observations and also to our interpreted mode of rapid transport. The upstream inclination of the long axis of the best-fit ellipsoid (Figure 8C, D) is similar to that commonly exhibited by grain flows and debris flows where the long axes parallel the flow direction and the b-c plane dips toward the source area (Leeder, 1982). The high angles of some clasts and some clast misalignment (data dispersion), likely reflects rapid deposition. The oblique orientation of the long axis of the best-fit ellipsoid with respect to the observed flow direction likely reflects either the use of only 3 planes of measurements or of depositional processes. Plane 3 (oblique to observed flow direction) has more data; thus, it likely influences the orientation of the long axis more than the less data rich plane 1 (parallel to observed flow direction). Furthermore, the oblique alignment of the long axis is common in rapid deposition of debris flows (Leeder, 1982).

On the basis of these observations we conclude that the basal shear zone formed after slope failure as the debris crossed the Brewster River and started to move across the adjacent terrace. Grain shape anisotropy in the basal shear zone formed as clay clasts

within a fluid-saturated matrix rotated into parallelism with the transport direction during rapid transport and rapid deposition. The degree of alignment is consistent with the observed flow direction and the relatively small (130 m) amount of slip at the exposure where we collected the strain data (70 m from the riverbank; Figure 3). The data also indicate that the basal layer experienced a greater amount of distortion compared to adjacent layers although clast rotation was the dominant deformation mechanism. We suggest that the occurrence of the saturated basal layer and processes operating within it explain why the debris runout length was so long.

*Mud volcanoes*

Within two days of the second slide, parts of the runout zone were covered with mud volcanoes of varying size (Figure 9). The central vents were saturated and liquefied with only slight agitation. The volcanoes were composed of gray silt similar to most of the debris. Subsequent excavation of the mud volcanoes did not confirm a sediment source; no feeder dikes were clearly visible. Thus, we are unable to ascertain explicitly the depth from which the mud volcanoes originated.

Mud volcanoes are most commonly associated with seismic shaking and are formed when fluid pore pressure is greater than the normal stress exerted by the overlying debris (Atwater, 1994; Obermeier, 1996; Obermeier *et al.*, 1992). There are only a few examples of non-seismic mud volcanoes caused by artesian conditions (Li *et al.*, 1996), filling of thermal contraction cracks (Pewe, 1959), sub-aqueous slumping (Gill and Keunen, 1958), and filling of ground cracks by sediment-laden surface run off (Holzer and Clark, 1993). Some have suggested that sub-aerial landsliding can produce mud volcanoes,

but until now such landslide induced mud volcanoes have yet to be reported (Obermeier, 1996; Obermeier *et al.*, 1992).

Mud volcanoes are important for understanding the long runout length of the Jeffersonville debris apron. During landsliding, vibrational energy or Coulomb failure of the sediment can increase pore water pressures to liquefaction level and liquefied debris can flow longer distances than nonliquified material (Iverson, 1997; Iverson *et al.*, 1997). Small experimental debris flows demonstrate that basal fluid pressures can exceed normal stresses and liquefy debris during deceleration and deposition. Such debris can remain liquefied for hours after deposition (Major and Iverson, 1999). Similarly, the Jeffersonville slides, composed of low permeability silt and clay, contained a liquefied basal layer, which dewatered slowly after deposition. The Jeffersonville landslide dewatered vertically through weak zones or fractures in the debris and formed mud volcanoes on the surface. Thus, the presence of the mud volcanoes is consistent with high basal pore pressures, liquefied debris, and the long runout distances of the Jeffersonville landslides.

## SLIDE MECHANICS

Distinctive features in the landslide scarp provide clues to the slide mechanics. Most prominent is an intact bench 5 meters above the Brewster River (Figure 6). The bench was the lower failure surface and a continuation of the bench can be seen both upstream and downstream of the landslide scar. The arcuate topographic profile suggests that the landslide was rotational (Figure 6).

*Failure initiation*

Most landslides in glacially conditioned terrains are caused by heavy precipitation or snowmelt increasing pore pressure (Gregersen and Sandersen, 1989; Iverson *et al.*, 1997; Niini and Slunga, 1989). In contrast, the Jeffersonville landslide occurred after six months when the average monthly precipitation was 2% below normal (Table II). Furthermore, there was less than 0.8 cm of precipitation in the week prior to the first landslide, April 11, 1999. These data indicate recent heavy or prolonged precipitation was not the direct cause of the landslides.

A mechanism other than recent precipitation initiated the landslides. Aerial photographs (1962, 1974, 1979, 1988, and 1995) suggest that river undercutting previously caused only minor sliding and slumping. The prominent bench 5-m above river level remains intact, suggesting that river undercutting and steepening of the bank were not the immediate cause of the 1999 landslides. Alternatively, focusing of shallow groundwater into a channel or gully can initiate landsliding by increasing local pore pressures (Montgomery, 1994); however, the very small size of the catchment above the slide (< 0.1 $km^2$) and absence of channels and gullies to focus groundwater flow argues against this initiation mechanism.

Landslides in fine-grained sediment are known to have a delayed response to heavy rainfall. The Minor Creek, California landslide, developed in clay, does not respond to individual storms. Rather, prolonged precipitation of 3 months or more is required to initiate movement, an observation supported by mathematical models (Iverson, 2000). A landslide in glacial lake sediments of alternating silt and clay in British

Columbia occurred during a dry period (Thompson and Mekechuk, 1982). The British Columbia landslide was initiated by a delay in groundwater response to precipitation as suggested by high artesian water pressures at the time of failure (Thompson and Mekechuk, 1982). We believe the slides at Jeffersonville are similarly triggered. A six month delay in groundwater response suggests that the heavy precipitation in the summer of 1998 (~175% of normal precipitation, Table II) was likely responsible for landslide initiation.

*Hillslope saturation*

In order to predict the extent of hillslope saturation at the time of failure, we determined the critical factor of safety (F = 1) using the Bishop method of slices (Bishop, 1955) and the soil parameters from the direct shear test (Table III). Additional shear vane tests (n = 66), measured both vertically and horizontally, revealed heterogeneous strengths within individual layers and along vertical sections of the bank (Figure 10). Although there is variability in shear vane results, generally the data suggest that the sediment above the bench has lower shear strength than the bench sediment (Figure 10), consistent with both the observation of failure at the bench and the soil cohesion results (Table III). Using the bench as a limit of failure plain depth, we determined a critical factor of safety (F=1) at 60% saturation of sediment above the concave failure plain. However, if conditions were artesian and groundwater saturated the hillslope from the below as we suspect, the failure would occur at lower values of saturation.

## IMPLICATIONS

Analysis of the Jeffersonville landslides has important implications for landslide occurrence and landslide hazard prediction throughout high latitudes. The 1999 landslides initiated during a six-month span in which the precipitation was below average. There was less than 0.8 cm of water input by rainfall during the week prior to initiation. An intact sediment bench indicates that river undercutting was not the direct cause of landsliding. It appears likely that a delayed pore pressure increase, forced by the deep bedrock system and transmitted through low permeability glaciolacustrine sediments, caused landsliding to lag heavy rainfall by six months.

Evidence from the debris zone, such as mud volcanoes, a 20-cm-thick basal shear zone, strain data, lobes at the slide margin, and the long runout distance suggests that the landslide mobilized and behaved like a debris flow. This allowed transport of sediment farther than would have been expected using similar volume landslides as a benchmark. The saturated basal shear zone aligned clay clasts as it deformed, facilitating the long runout. The saturated slide mass became a source for mud volcanoes that formed on the debris surface. Although some landslides mobilize into debris flows, few hazard maps consider this phenomena. The Jeffersonville slides provide compelling evidence that landslide hazard delineation should compensate for such behavior.

## ACKNOWLEDGMENTS

K. Jennings and G. Fredrickson helped in data collection. J. Olson, University of Vermont, Civil Engineering assisted in shear strength measurements. Research supported

by National Science Foundation CAREER grant EAR - 9702643 to Bierman. GPS gear funded through MRI EAR 9724190 to Bierman and Lini.

**REFERENCES CITED**

Atwater BF. 1994. *Geology of Holocene liquefaction features along the Lower Columbia River at Marsh, Brush, Price, Hunting, and Wallace Islands, Oregon and Washington*. U.S. Geological Survey Open File Report 94-209: Reston, Virginia.

Bathurst JC, Burton A, Ward TJ. 1997. Debris flow run-out and landslide sediment delivery model tests. *Journal of Hydraulic Engineering* **123**:410-419.

Bishop AW. 1955. The use of the slip circle in the stability analysis of earth slopes. *Geotechnique* **5**:7-17.

Brabb EE. 1989. Landslides: Extent and Economic Significance. In *The 28th International Geological Congress: Symposium on Landslides*. Washington D.C.

Braun DD, Gillmeister NM, Inners JD. 1989. Post-glacial to historic dip-slope block slides in the Valley and Ridge province of northeastern Pennsylvania. In *Landslide processes of the eastern United States and Puerto Rico. Special Paper 236,* Schultz AP, Jibson RW (eds). Geological Society of America: Boulder, Colorado:75-87.

Campbell CS. 1989. Self-lubrication for long runout landslides. *The Journal of Geology* **97**:653-665.

Campbell CS, Cleary PW, Hopkins M. 1995. Large-scale landslide simulations: Global deformation, velocities and basal friction. *Journal of Geophysical Research* **100**(B5):8267-8283.

Chapman DH. 1937. Late glacial and post-glacial history of the Champlain Valley. *American Journal of Science* **34**:89-124.

Dade WB, Huppert HE. 1998. Long-runout rockfalls. *Geology* **26**:803-806.

De Paor DG. 1988. Rf/phi strain analysis using an orientation net. *Journal of Structural Geology* **10**:323-333.

Dunne T, Leopold LB. 1978. *Water in environmental planning.* W. H. Freeman: San Francisco.

Flemming RW, Ellen SD, Algus MA. 1989. Transformation of dilative and contractive landslide debris into debris flows-An example from Marin County, California. *Engineering Geology* **27**:201-223.

Gill WD, and Keunen PH. 1958. Sand volcanoes on slumps in the Carboniferous of County Clare, Ireland. *Quarterly Journal of the Geological Society of London* **113**:441-460.

Gregersen O, and Sandersen F. 1989. Landslide: Extent and economic significance in Norway. In *Landslides: Extent and economic significance.* Brabb EE, Harrod BL (eds). A.A. Balkema: Rotterdam:133-139.

Holzer TL, Clark MM. 1993. Sand boils without earthquakes. *Geology* **21**:873-876.

Hsü KJ. 1975. On Sturzstroms-Catastrophic debris streams generated by rockfalls. *Geological Society of America Bulletin* **80**:129-140.

Iverson RM. 1997. The physics of debris flows. *Reviews in Geophysics* **35**:245-296.

Iverson RM. 2000. Landslide triggering by rain infiltration. *Water Resources Research* **26**(7):1897-1910.

Iverson RM, Reid ME, LaHusen RG. 1997. Debris-flow mobilization from landslides. *Annual Review of Earth and Planetary Science* **25**:85-138.

Johnson AM. 1984. Debris flow. In *Slope Instability.* Brunsden D, Prior DB (eds). Wiley: London:257-361.

Kilburn CRJ, Sørensen SA. 1998. Runout lengths of sturzstroms: The control of initial conditions and of fragment dynamics. *Journal of Geophysical Research* **103**(B8):17,877-17,884.

Koteff C, Pessell S. 1981. *Systematic ice retreat in New England, USGS Professional Paper 1179.* US Government Printing Office: Washington D.C.

Leeder MR. 1982. *Sedimentology, process and product*. Allen and Unwin Inc.: Wincheser, Mass.

Li Y, Craven, J., Schweig ES, Obermeier SF. 1996. Sand boils induced by the 1993 Mississippi River flood: Could they one day be misinterpreted as earthquake-induced liquefaction? *Geology* **24**:171-174.

Lisle RJ. 1985. *Geological strain analysis a manual for the $R_f/\Phi$ method*. Pergamon Press: Oxford.

Major JJ, Iverson RM. 1999. Debris-flow deposition: Effects of pore-fluid pressure and friction concentrated at flow margins. *Geological Society of America Bulletin* **111**:1424-1434.

Mollard JD. 1977. Regional landslide types in Canada. In *Landslides: Reviews in Engineering Geology.* Coates DR (ed). The Geological Society of America: Boulder Colorado:29-56.

Montgomery DR. 1994. Road surface drainage, channel initiation, and slope instability. *Water Resources Research* **30**(6):1925-1932.

Nayashi JN, Self S. 1992. A comparison of pyroclastic flow and debris flow mobility. *Journal of Geophysical Research* **97**(B6):9063-9071.

Niini H, Slunga E. 1989. Landslides in Finland. In *Landslides: extent and economic significance.* Brabb EE, Harrod BL (eds). A.A. Balkema: Rotterdam: 149-151.

Obermeier SF. 1996. Use of liquefaction-induced features for paleoseismic analysis - An overview of how seismic liquefaction features can be distinguished from other features and how their regional distribution and properties of source sediment can be used to infer the location and strength of Holocene paleo-earthquakes. *Engineering Geology* **44**:1-76.

Obermeier SF, Martin JR, Frankel AD, Youd TL, Munson PJ, Munson CA, Pond EC. 1992. *Liquefaction evidence for strong Holocene earthquake(s) in the Wabash Valley of southern Indiana-Illinois, with a preliminary estimate of magnitude*. U.S. Geological Survey: Reston, Virginia 92-406.

Owens WH. 1984. The calculation of a best-fit ellipsoid from elliptical sections on arbitrarily oriented planes. *Journal of Structural Geology* **6**:571-578.

Pewe TL. 1959. Sand-wedge polygons (tessellations) in the McMurdo Sound region, Antarctica - A progress report. *American Journal of Science* **257**:545-551.

Thompson S, Mekechuk J. 1982. A landslide in glacial lake clays in central British Columbia. *Canadian Geotechnical Journal* **19**:296-306.

Viberg L. 1989. Extent and economic significance of landslides in Sweden. In *Landslides: extent and economic significance.* Brabb EE, Harrod BL (eds). A.A. Balkema: Rotterdam:141-147.

**FIGURE CAPTIONS**

Figure 1. Landslide locations at Jeffersonville, Vermont. Grey lines show locations of 1999, 1962, and undated landslide scars. Base is 1979 Jeffersonville orthophoto, sheet no.124236. White contours from 1:24,000 USGS Jeffersonville, Vermont quadrangle (1948). Inset shows Jeffersonville (J) location.

Figure 2. Photographs of the failed slope that caused the Jeffersonville landslides. A) Photograph taken in 1910 or 1911. Lower arrow points to unvegetated areas where small slides and slumping were occurring. Area of 1999 slide is indicated by upper arrow and appears unstable. B) Photograph taken in 2000 from near the same location as earlier photograph. The Jeffersonville landslides occurred in an area that was unvegetated in the earlier photograph. Field of view for both photographs is ~ 1 km.

Figure 3. Topographic map of runout zone (gray) from data collected (> 3000 points) using Trimble 4400 real-time kinematic GPS after the second landslide, April 18, 1999. Contour interval changes from 0.5 m to 2.0 m above 150 m. Brewster River is black. Letters A through D denote debris flow snouts at slide margin, and associated cross sections inset above. Numbers on cross sections represent individual superimposed debris flow lobes. Large mud volcano field (Figure 9B) is located at "X". Largest mud volcano (Figure 9A) is located at "Y". Clast alignment data collected at "Z". A to A' is location of cross section in Figure 6.

Figure 4. Photograph of debris zone. Blocks of sediment are composed of rigid silt/clay couplets. Trees were on slope prior to failure and were transported with slide debris.

Figure 5. Orientations of fallen and tilted trees on the slide mass are bimodal. Histograms show orientation difference between A) slide margin and trees within 20 m of the slide margin and B) local flow direction and trees more than 20 m from slide margin. Trees at slide margin were pushed along by debris. Trees more than 20 m from slide margin fell along radial paths during transport.

Figure 6. Cross-section of cutbank and debris zone. L is the total runout length of debris (290 m), $L_m$ is distance to the center of mass runout of the debris (140 m), H is the total drop height (46 m), $H_m$ is the center of mass drop height (20 m). Pre-landslide topography is assumed to be similar to measured topography at scarp margins. Post-slide topography (data collected after second slide) shows presence of bench. Because of unstable and dangerous slope, cross-sectional survey data do not fully depict bench. Slide material is shaded gray. Top 4 m of hillslope is sand and gravel.

Figure 7. Graph of landslide volume vs. H/L (after Kilburn and Sørensen, 1998). Data represent landslides from the Moon, Mars, and Earth. The Jeffersonville slide (denoted by star) has a long runout for its volume. Dashed lines represent upper and lower envelopes of typical H/L ratios for landslides.

Figure 8. A) Basal (20 cm) shear zone in cross-section. Buried grass surface is visible and intact indicating non-erosive transport. Small (~2 cm), angular clay clasts (indicated by arrows) in a silty matrix characterize the shear zone. Overlying vertical section exhibits intact rhythmites with some folding and faulting. Flow direction of debris is toward reader. B) Plots of clast shape ($R_f$) vs. angle of inclination. Plane 1 strikes 085 and positive phi is to the E. Plane 2 strikes N-S, positive phi is to the N. Plane 3 strikes 326, positive phi is to the NW. Average $R_f$ and phi values are represented by dotted lines. C) Equal-Area lower hemisphere stereoplot showing the orientation of the best-fit ellipsoid to clast shape (Rf) and preferred orientation (phi) data. Flow plane is horizontal surface. Observed flow direction is denoted by gray arrow. D) 2-D vertical section of x-z plane taken parallel to observed flow direction denoted by arrow. Clasts dip toward source area, consistent with debris flow behavior and a basal shear zone.

Figure 9. Mud volcanoes. A) Large mud volcano at location “Y” on Figure 3. Central vent is ~20 cm wide; apron is >1 m in diameter. B) Field of mud volcanoes with slide scar in background at "X" on Figure 3.

Figure 10. Horizontal (circles) and vertical (squares) shear vain data. Bench is at 150 m elevation. Limit curve (dashes) shows the bench is more cohesive and thus stronger than overlying strata.

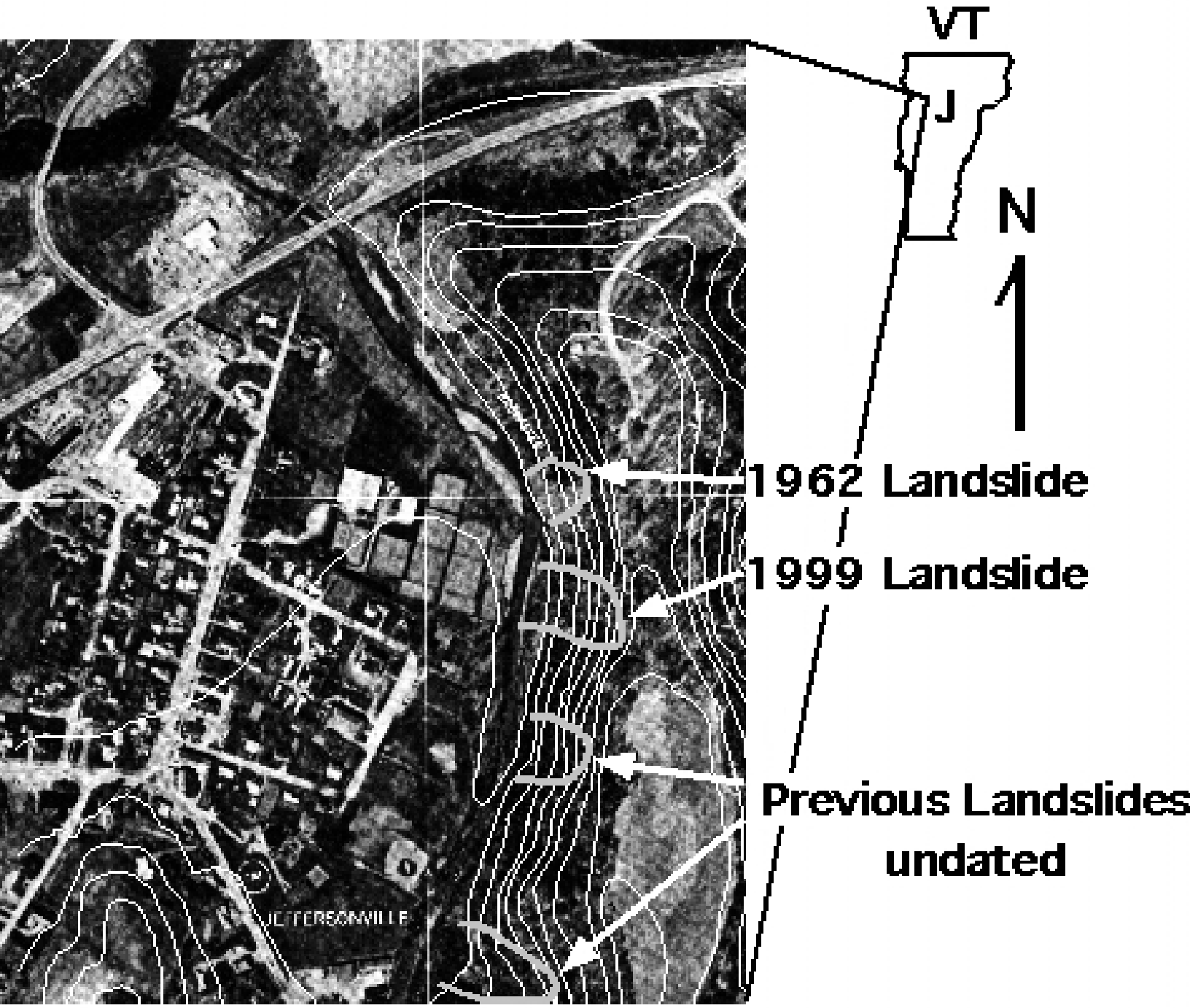


Nichols et al. Fig. 1

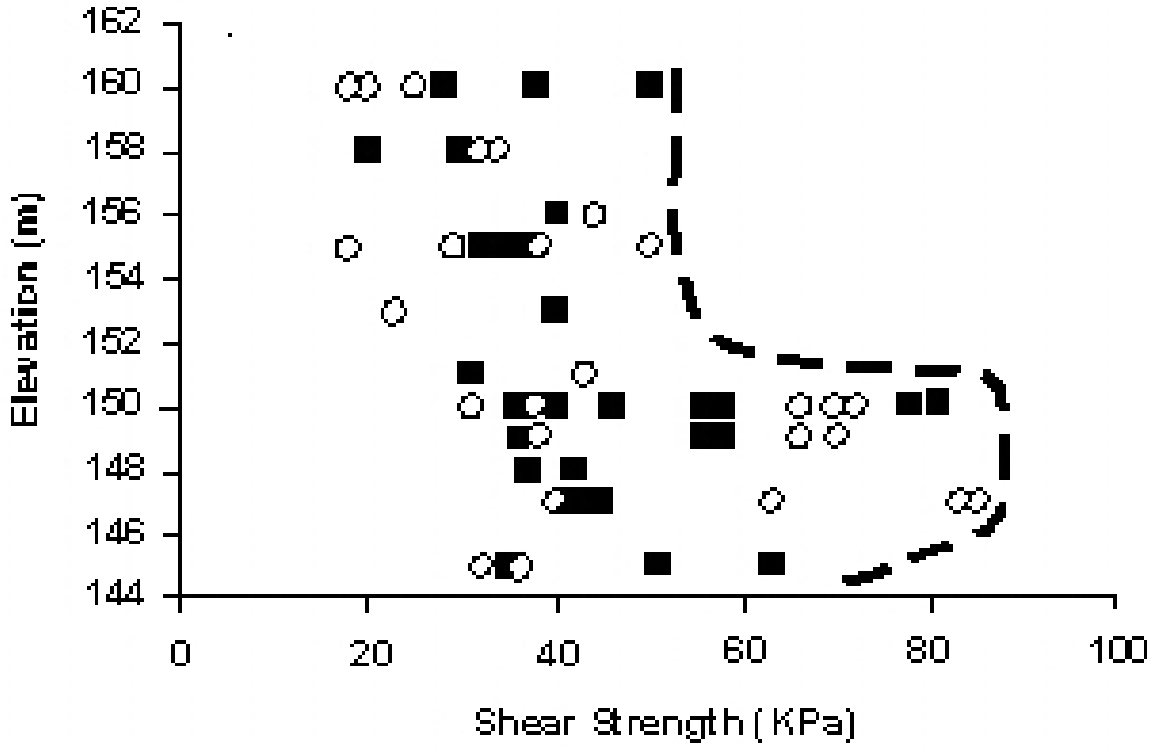


Nichols et al. Fig. 10

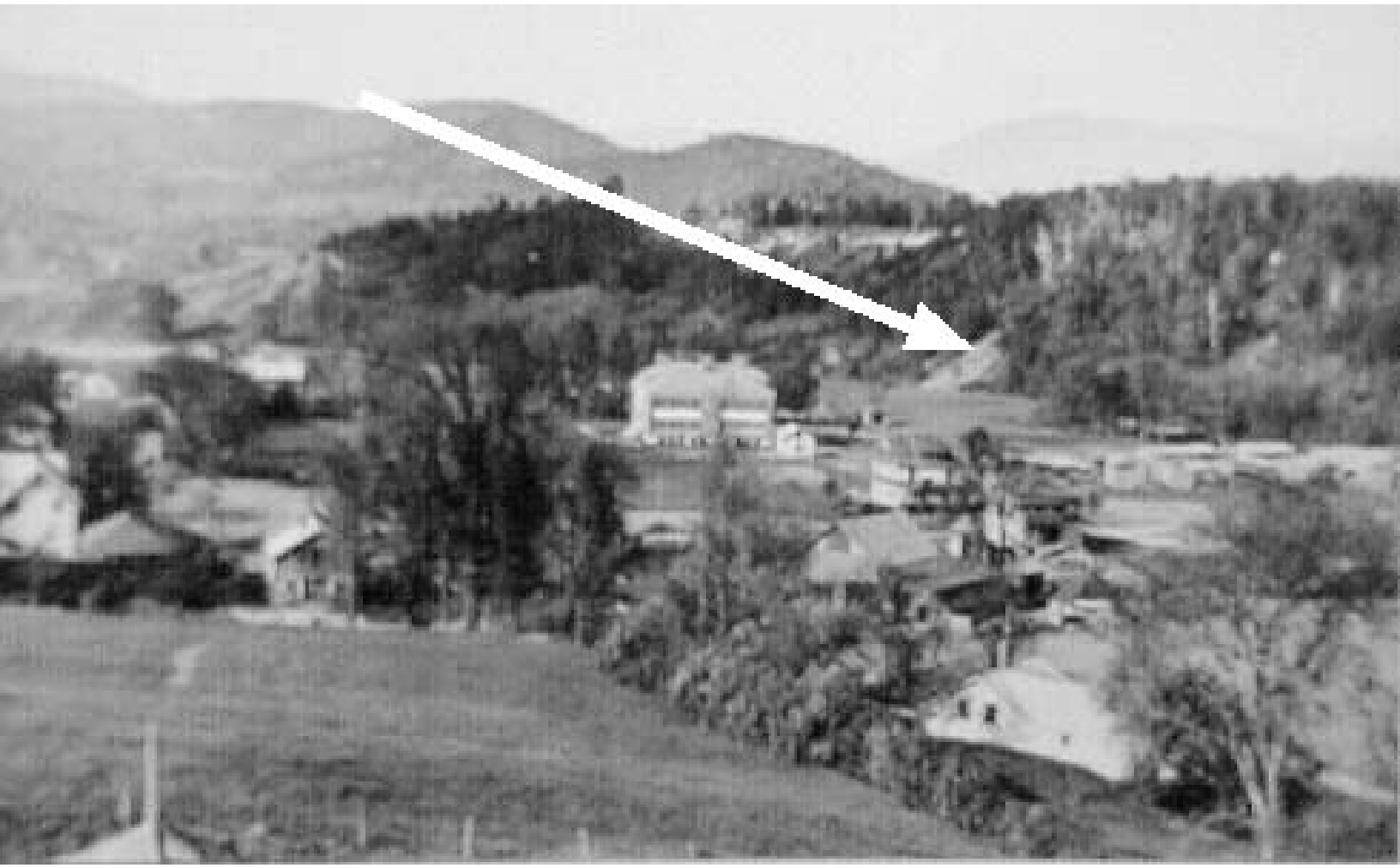

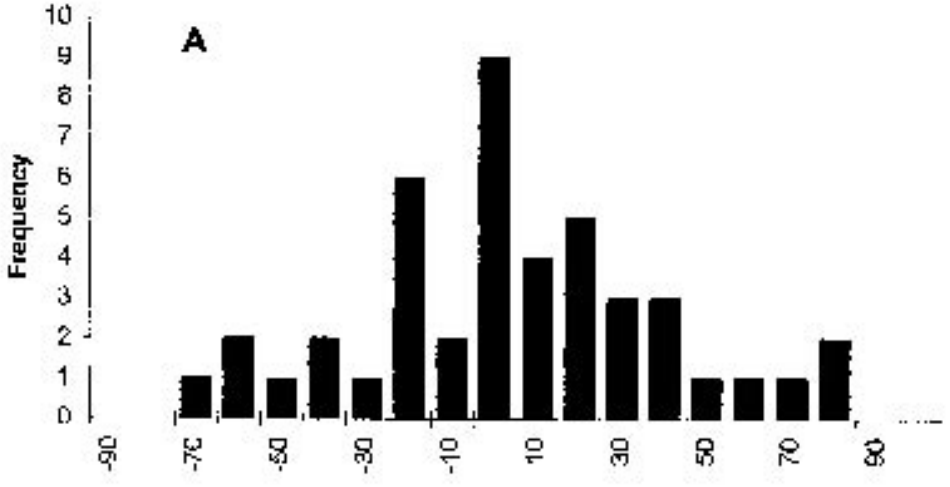


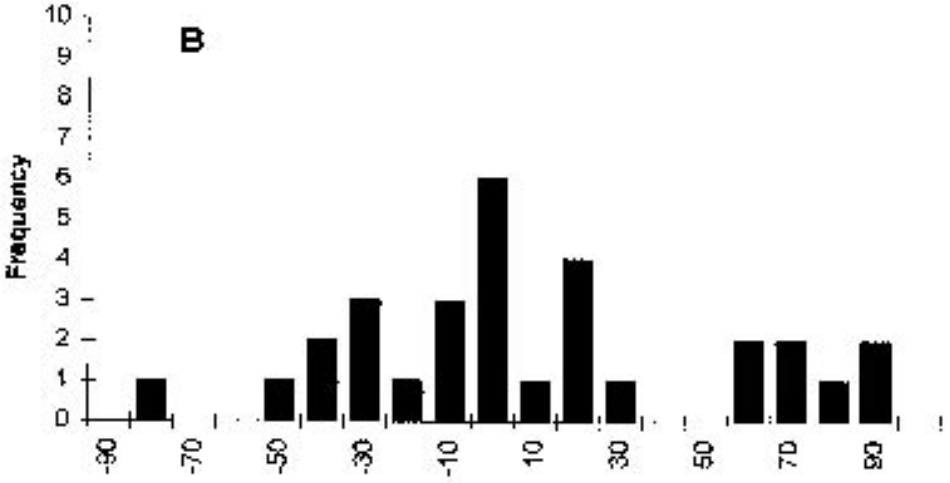


Nichols et al. Fig. 4

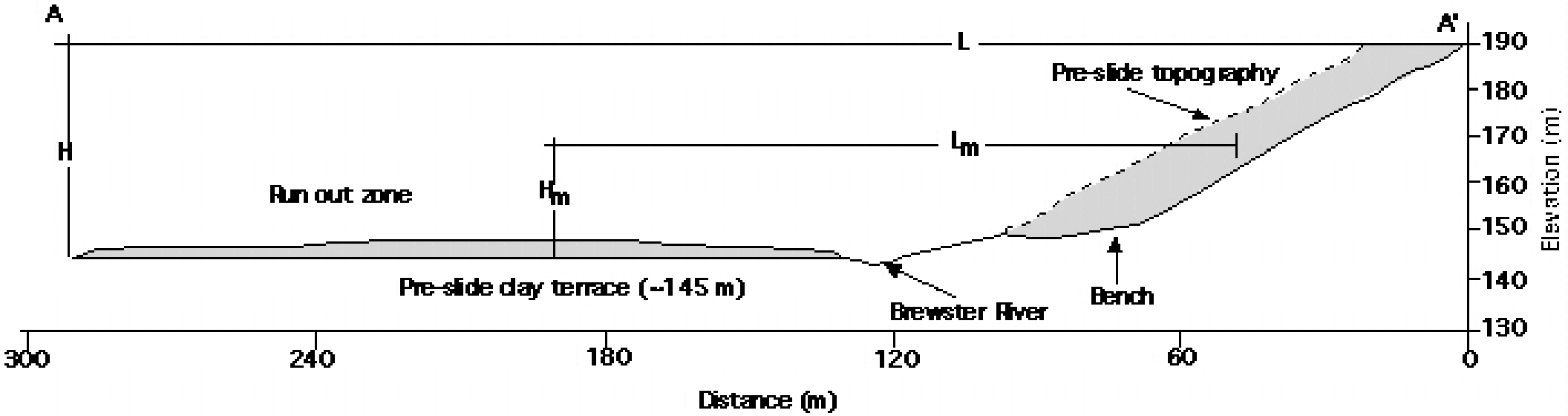
A
A'
L
H
$L_m$
$H_m$
Run out zone
Pre-slide topography
Pre-slide clay terrace (~145 m)
Brewster River
Bench
190
180
170
160
150
140
130
Elevation (m)
300
240
180
120
60
0
Distance (m)

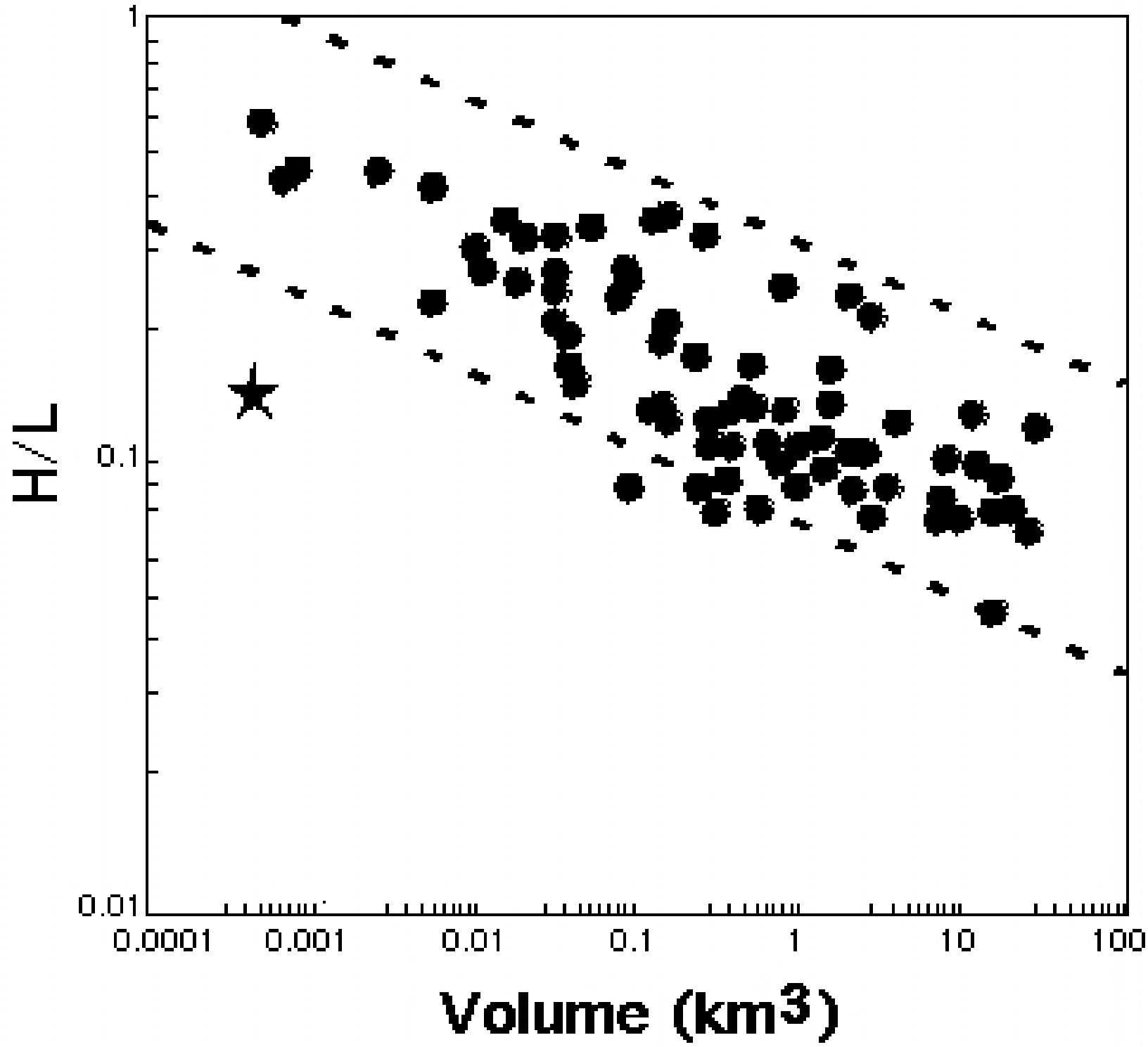
1
0.1
0.01
H/L
0.0001
0.001
0.01
0.1
1
10
100
Volume (km3)

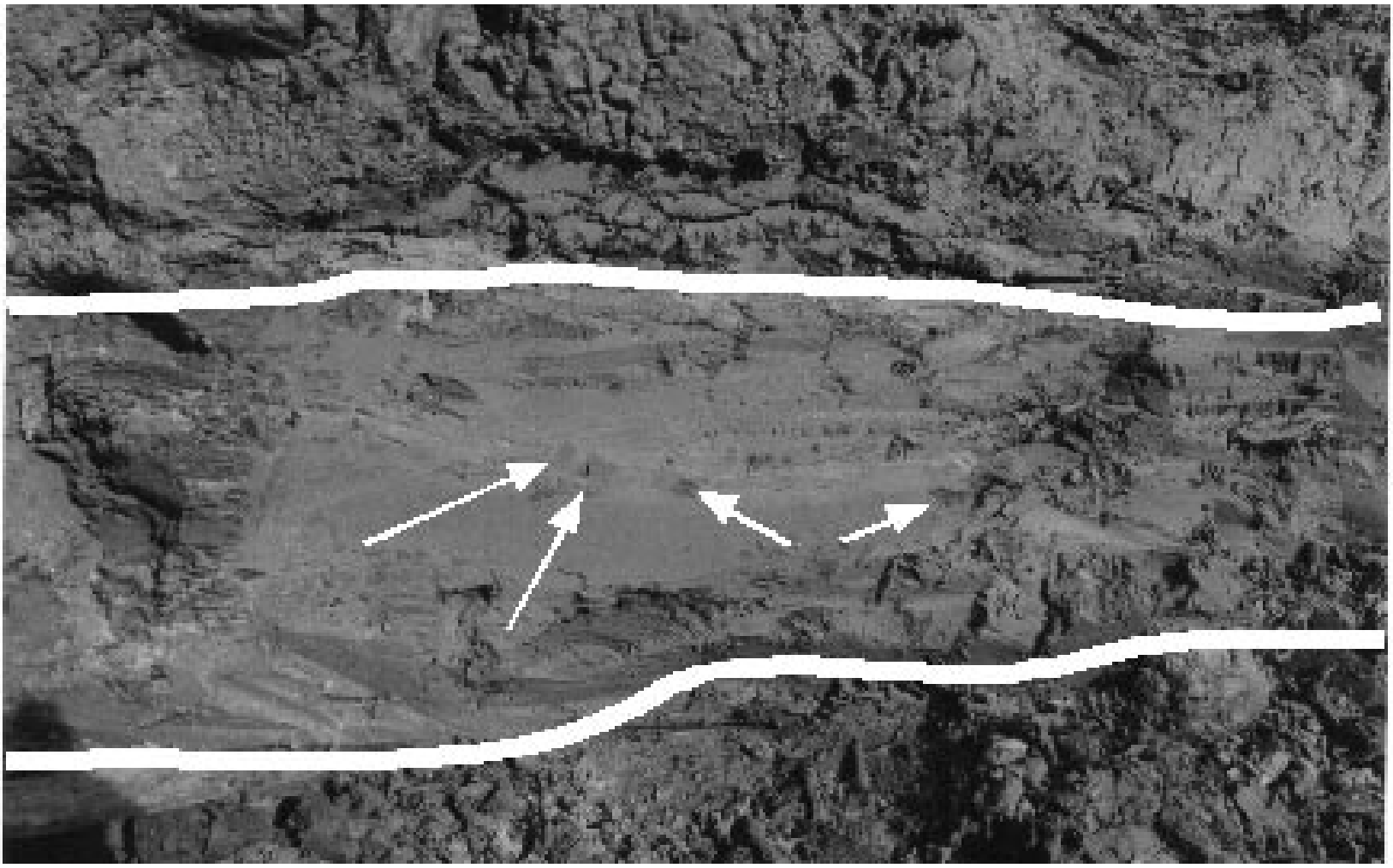

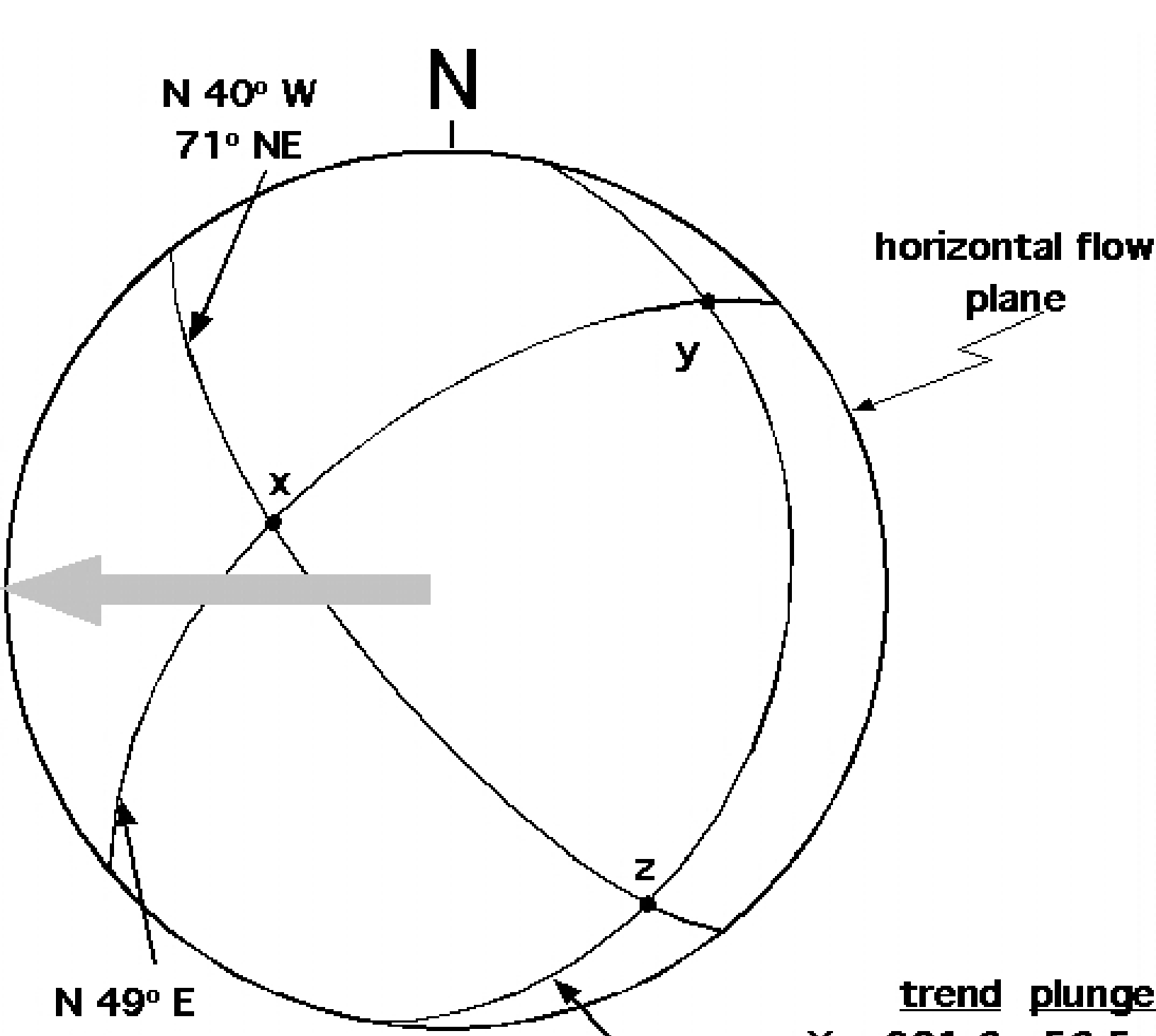


| | trend | plunge |
|---|---|---|
| X = | 281.6 | 56.5 |
| Y = | 42.5 | 18.8 |
| Z = | 142.3 | 26.7 |

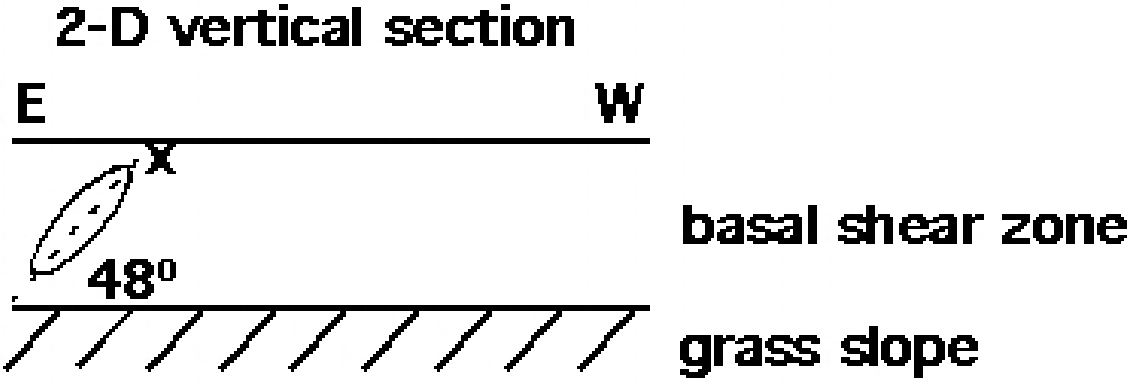

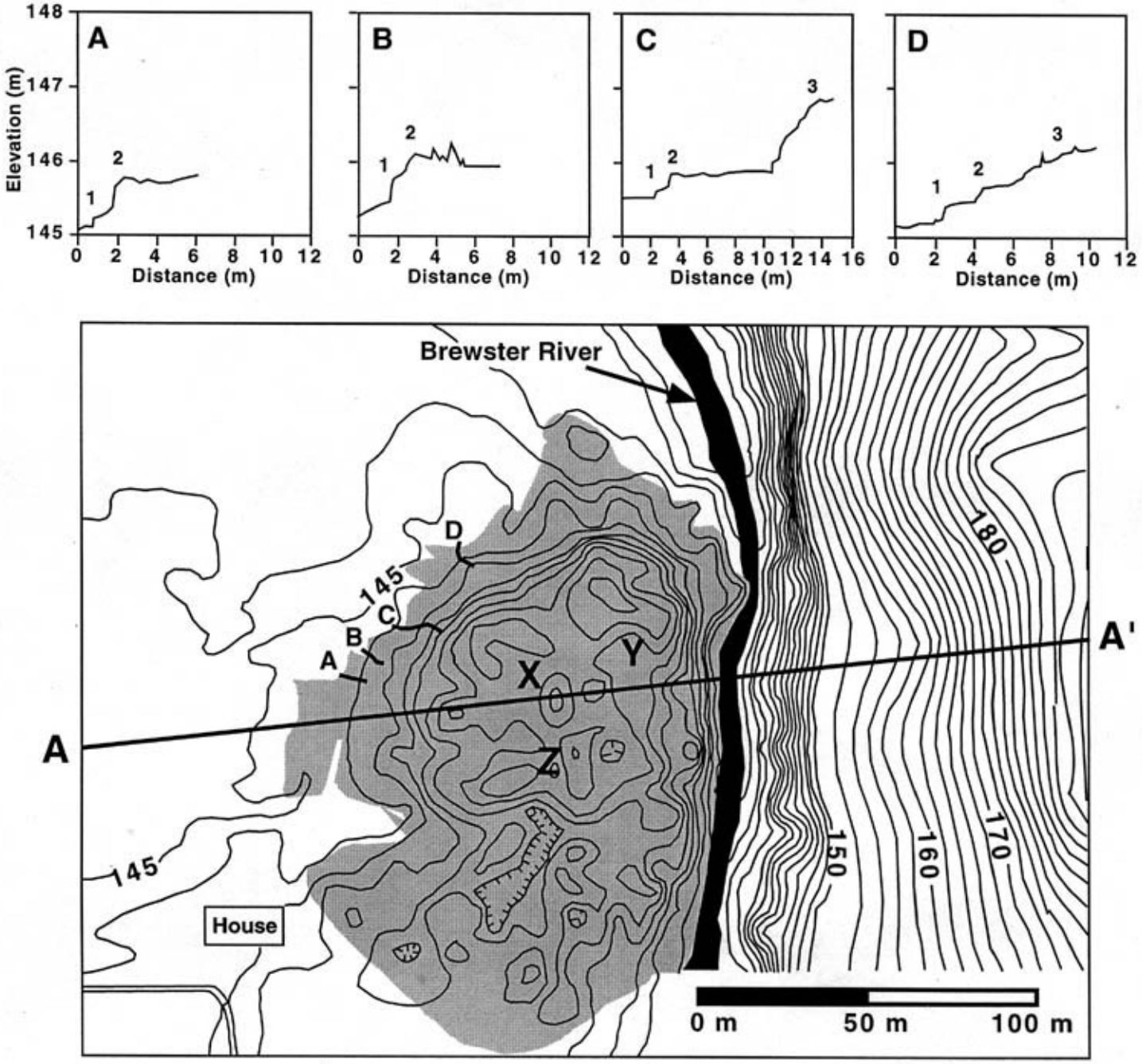


Nichols et al. Figure 3

Table I. Runout lenghts of landslides and debris flows

| Source | Type of material | Equation[a] | Distance[b] (m) |
|---|---|---|---|
| Campbell et al. (1995) | Granular landslide | H/L = 0.45 | 102 |
| Kilburn and Sørensen (1998) | Granular landslide | H/L = 0.35 | 131 |
| Ikeya (1981) | Debris flow | $L = 8.6(V \tan \Theta)^{0.42}$ | 565 |
| Bathurst et al. (1997)[c] | Debris flow | $L = 25\ V^{0.3}$ | 515 |
| Bathurst et al. (1997)[d] | Debris flow | $\tan \alpha = 0.2$ | 230 |
| This paper | Debris flow-like behavior | observation | 290 |

[a]Jeffersonville slide: H = 46 m based on total drop, V = 23,000 $m^3$, $\Theta = 29°$, $\tan \alpha = H/L$

[b]Predicted run out distance for second Jeffersonville landslide.

[c]Bathurst personal communication with Rickenmann (1994)

[d]Bathurst personal communication with Takahashi (1994)

TableII Monthly precipitation for Morrisville and Burlington, Vermont from June 1998 to June 1999

| Period | Year | Month | Morrisville[a] | Burlington[b] | Burlington average[c] | Percent change[d] |
|---|---|---|---|---|---|---|
| Wet | 1998 | June | 21.8 | 22.0 | 8.8 | 148 |
| | | July | 21.2 | 23.6 | 9.3 | 128 |
| | | August | 12.8 | 17.3 | 10.3 | 24 |
| | | September | 10.9 | 14.3 | 8.4 | 31 |
| ***Total change*** | | | | | | ***+83*** |
| Dry | | October | 5.7 | 6.1 | 7.3 | -22 |
| | | November | 6.4 | 2.6 | 8.0 | -20 |
| | | December | 3.3 | 0.9 | 6.1 | -46 |
| | 1999 | January | 13.5 | 8.9 | 4.6 | 192 |
| | | February | 3.1 | 2.9 | 4.1 | -25 |
| | | March | 8.6 | 5.6 | 5.7 | 52 |
| | | April | 1.3 | 1.9 | 7.0 | -82 |
| | | May | 6.8 | 6.1 | 7.9 | -14 |
| | | June | 9.7 | 4.5 | 8.8 | 10 |
| ***Total change*** | | | | | | ***-2*** |

[a]Morrisville is the closest precipitation gauge to Jeffersonville, record is not long enough to get annual average precipitation.

[b]Burlington is the closest location (??km) to Jeffersonville with an annual average precipitation. Morrisville and Burlington precipitation are well correlated for June 1998 to June 1999 ($r^2 = 0.82$)

[c]Annual average precipitation at Morrisville is probably 5 cm higher based on elevation.

[d]Based on Morrisville precipitation compared to Burlington average.

Table III Direct shear test data

| Sample location | Elevation (m) | Soil cohesion (kPa) | Internal angle of friction (°) |
|---|---|---|---|
| Below bench | 146 | 8.2 | 28 |
| Top of bench | 150 | 17 | 22 |
| Above bench | 154 | 5.6 | 38 |